

Asymmetric hydrogenation by $\text{RuCl}_2(\text{R-Binap})(\text{dmf})_n$ encapsulated in silica-based nanoreactors†

Cite this: DOI: 10.1039/c4cy00228h

Juan Peng,^{ab} Xuefeng Wang,^a Xiaoming Zhang,^{ab} Shiyang Bai,^a Yaopeng Zhao,^a Can Li^{*a} and Qihua Yang^{*a}

The Noyori catalyst $\text{RuCl}_2(\text{R-Binap})(\text{dmf})_n$ has been successfully encapsulated in C-FDU-12 by using the active chlorosilane $\text{Ph}_2\text{Cl}_2\text{Si}$ as the silylating agent. ³¹P-NMR results show that there is no strong interaction between the molecular catalyst and the solid support, thus the encapsulated molecular catalyst could move freely in the nanoreactor during the catalytic process. The solid catalyst exhibits high activity and enantioselectivity for the asymmetric hydrogenation of a series of β -keto esters due to the preserved intrinsic properties of $\text{RuCl}_2(\text{R-Binap})(\text{dmf})_n$ encapsulated in the nanoreactor. The solid catalyst could be recycled by simple filtration and be reused at least four times.

Received 20th February 2014,
Accepted 12th April 2014

DOI: 10.1039/c4cy00228h

www.rsc.org/catalysis

Introduction

Asymmetric catalysis is one of the most efficient approaches for the production of chiral chemicals. Over the past decades, huge progress has been made for homogeneous asymmetric catalysis. Versatile and efficient asymmetric catalytic systems have been developed for the synthesis of various enantiomers which are important in both fine-chemical and pharmaceutical industries.^{1–5} From the viewpoint of industrial application, it is desirable to produce chiral compounds through the heterogeneous asymmetric catalytic approach due to its overwhelming advantages in recycling and reuse of the expensive homogeneous asymmetric catalysts, easy purification of the products and convenient manipulation for large scale production.

However, heterogeneous asymmetric catalysts which are often prepared by simple immobilization of homogeneous asymmetric catalysts onto solid supports always face the problems of low enantioselectivity and catalytic activity.^{6,7} This is partly because the molecular catalysts lose their mobility after immobilization, which may alter their intrinsic properties. Great efforts have been made in trying to keep the intrinsic properties of molecular catalysts after immobilization; for example, encapsulating the metal complex catalyst in a zeolite through the “ship-in-bottle” method.^{8–10} Unfortunately, the small pore size of zeolites and the uncontrollable coordination process

within pores have restricted their application for more complicated catalysts. Recently, our group has developed an efficient strategy to encapsulate molecular catalysts in silica-based nanoreactors with cage-like porous structures, such as SBA-16 and FDU-12, by post-modification of the pore entrance through a silylation method. With this method, several types of metal complex catalysts, such as $\text{Co}(\text{Salen})$,^{11–13} $\text{VO}(\text{Salen})$,¹⁴ $\text{Fe}(\text{Salen})$,¹⁵ $\text{Cr}(\text{Salen})$,¹⁶ $\text{Ru}(\text{Ts-DPEN})$ ¹⁷ and $(\text{Binolate})_2\text{Ti}$ ¹⁸ have been successfully trapped in the nanocages of mesoporous materials. It has also been demonstrated that the encapsulated molecules could move freely in the nanoreactor based on ³¹P-NMR characterization using BINAPO (2,2'-bis(diphenylphosphino)oxide-1,1'-binaphthyl) as the model molecule.¹³ The catalytic performance of the encapsulated molecular catalysts is comparable to, and in some cases even higher than, those of the homogeneous counterparts.

Our previous encapsulation method always required an organic base, such as pyridine, as a silylation catalyst during the silylation process to reduce the pore entrance size. However, due to its strong coordination ability, pyridine may deteriorate some metal complexes. It is therefore desirable to develop new methods for the encapsulation of special types of catalysts, for example, $\text{RuCl}_2(\text{R-Binap})(\text{dmf})_n$ (abbreviated as Ru-(R-Binap) in the following paragraphs; as for the structural formula, $\text{RuCl}_2(\text{R-Binap})(\text{dmf})_2$ ($n = 2$) is taken as the representative), which has been widely used in asymmetric hydrogenation after being reported by Noyori and Takaya in 1980.¹⁹ Ru-(R-Binap) is air sensitive and loses its catalytic activity in the presence of pyridine. Many efforts have been made to immobilize Binap onto different types of supports, such as zirconium phosphonate,^{20,21} Fe_3O_4 ,^{22,23} PMOs,²⁴ graphite oxide,²⁵ polymers,²⁶ ionic liquids,^{27–29} etc.; however, the immobilization of Ru-(R-Binap) through non-covalent interactions

^a State Key Laboratory of Catalysis, Dalian Institute of Chemical Physics, Chinese Academy of Sciences, 457 Zhongshan Road, Dalian 116023, China. E-mail: yangqh@dicp.ac.cn, canli@dicp.ac.cn; Fax: +86 0411 84694447

^b Graduate School of the Chinese Academy of Sciences, Beijing 100049, China

† Electronic supplementary information (ESI) available. See DOI: 10.1039/c4cy00228h

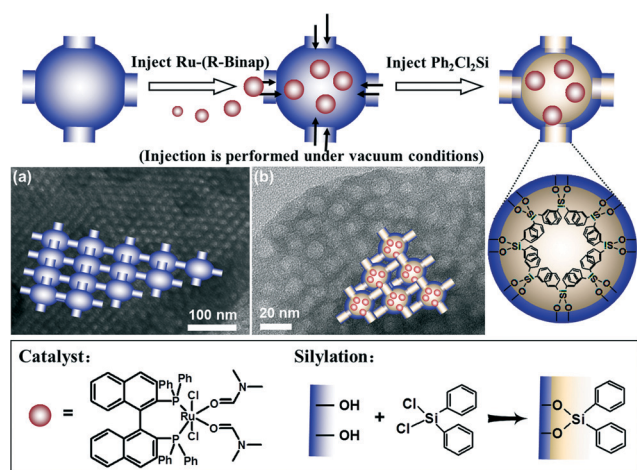
has rarely been reported. Herein, we describe a new method for encapsulating this organic base sensitive catalyst in the nanocages of mesoporous silica C-FDU-12 without deteriorating its activity. Based on the characterization results of nitrogen adsorption-desorption analysis, XRD and TEM, the ordered mesoporous structure of the cage-like material is maintained after the encapsulation of Ru-(*R*-Binap). Furthermore, ^{31}P -NMR spectroscopic studies show that the encapsulated Ru-(*R*-Binap) could move freely in the nanocages, which was seldom reported by other immobilization methods. To evaluate the catalytic performance of Ru-(*R*-Binap)@C-FDU-12, the asymmetric hydrogenation of β -keto esters was chosen as the model reaction. The influence of the loading amount of Ru-(*R*-Binap) on the catalytic performance of Ru-(*R*-Binap)@C-FDU-12 and the cycling stability of Ru-(*R*-Binap)@C-FDU-12 were also investigated.

Results and discussion

Encapsulation of the Ru-(*R*-Binap) complex in the nanocage of C-FDU-12

As illustrated in Scheme 1, Ru-(*R*-Binap) was first introduced into the nanocage of C-FDU-12 (obtained by carbonization of the as-made FDU-12 at 550 °C under a nitrogen atmosphere for 6 h, the carbon content is 4.8 wt%, Fig. 1b) under vacuum. Then the pore entrance size was reduced using $\text{Ph}_2\text{Cl}_2\text{Si}$ as the silylating agent at room temperature under vacuum. After being thoroughly washed with dichloromethane in a glove box, the solid catalyst, Ru-(*R*-Binap)@C-FDU-12, was obtained. In this case, we chose the very active chlorosilane $\text{Ph}_2\text{Cl}_2\text{Si}$ ³⁰ instead of alkoxysilanes as the silylating agent, thus the silylation could be performed at room temperature without any silylation catalysts. This will help in keeping the intrinsic properties of Ru-(*R*-Binap) during the encapsulation process.

FT-IR spectra of Ru-(*R*-Binap) and Ru-(*R*-Binap)@C-FDU-12 are presented in Fig. 2. Ru-(*R*-Binap)@C-FDU-12 displays the characteristic vibration bands of Ru-(*R*-Binap) at 3050 cm^{-1} ,



Scheme 1 Schematic illustration of encapsulating Ru-(*R*-Binap) in the nanocage of C-FDU-12 and TEM images of C-FDU-12 (a) before and (b) after encapsulation of Ru-(*R*-Binap).

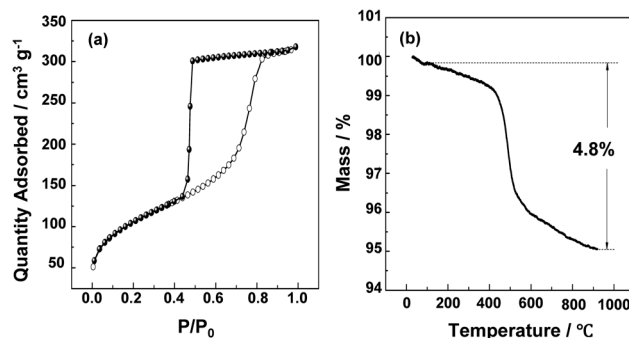


Fig. 1 (a) The N_2 sorption isotherm and (b) the TG curve of C-FDU-12.

810 cm^{-1} , 743 cm^{-1} , 697 cm^{-1} for C(naphthalene)-H, and 1434 cm^{-1} for P-C(aryl). The UV-vis diffused reflectance spectrum of Ru-(*R*-Binap)@C-FDU-12 clearly shows the bands at 338 nm, similar to that of Ru-(*R*-Binap) dissolved in CH_2Cl_2 (Fig. S3†). The results of FT-IR and UV-vis spectroscopy confirm the successful encapsulation of Ru-(*R*-Binap) in the nanocage of C-FDU-12.

Textural properties of Ru-(*R*-Binap)@C-FDU-12

The N_2 sorption isotherms of Ru-(*R*-Binap)@C-FDU-12 are of type IV with an H2 hysteresis loop similar to that of parent C-FDU-12, indicating that the solid catalyst still maintains the cage-like porous structure (Fig. 1a and 3A). In comparison with C-FDU-12, an obvious decrease in the BET surface area and cage size is observed due to the occupation of the Ru-(*R*-Binap) catalyst in the nanocages (Table 1). As the content of Ru-(*R*-Binap) increases, the BET surface area and pore volume of Ru-(*R*-Binap)@C-FDU-12 decrease gradually.

The XRD patterns of Ru-(*R*-Binap)@C-FDU-12 (0.71 wt% Ru) exhibit two well-resolved diffraction peaks (Fig. 3B), which can be indexed to the (111) and (311) reflections of a fcc structure (*Fm*3*m*),³¹ similar to C-FDU-12. The TEM images also show that the ordered distribution of the mesopores of C-FDU-12 remains invariable after the encapsulation of Ru-(*R*-Binap) (Scheme 1). The above results confirm that Ru-(*R*-Binap)@C-FDU-12 has a

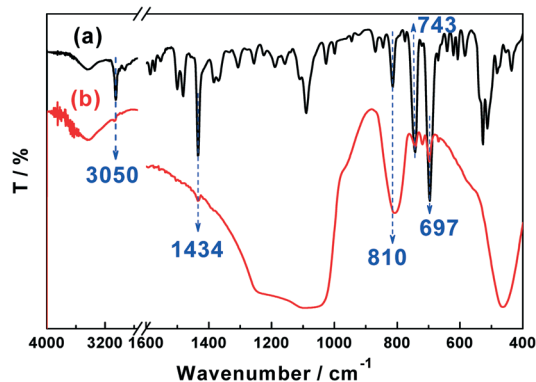


Fig. 2 FT-IR spectra of (a) Ru-(*R*-Binap) and (b) Ru-(*R*-Binap)@C-FDU-12 (0.71 wt% Ru).

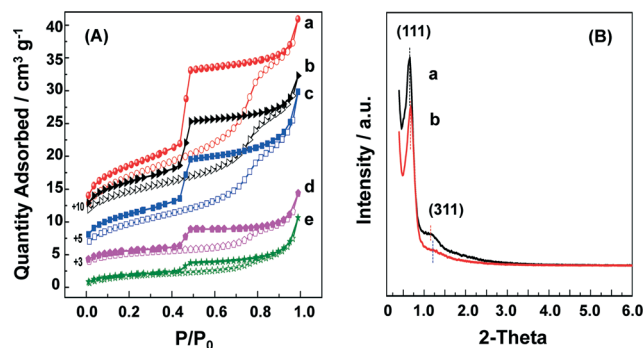


Fig. 3 (A) The N_2 sorption isotherms of Ru-(*R*-Binap)@C-FDU-12 at different Ru content: (a) 0.12 wt%, (b) 0.28 wt%, (c) 0.37 wt%, (d) 0.5 wt% and (e) 0.71 wt%. (B) XRD patterns of (a) C-FDU-12 and (b) Ru-(*R*-Binap)@C-FDU-12 (0.71 wt% Ru).

well ordered cage-like porous structure and the encapsulation of Ru-(*R*-Binap) does not damage the porous structure of C-FDU-12.

Investigation of the movement freedom of Ru-(*R*-Binap) encapsulated in C-FDU-12

In our previous work, the degree of movement freedom of the molecule encapsulated in the nanocages of mesoporous silica was detected using BINAPO (2,2'-bis(diphenylphosphino)oxide)-1,1'-binaphthyl) as a model molecule.¹³ However, the movement freedom of the real catalysts was not detected. In this work, the movement freedom of the molecular catalyst, Ru-(*R*-Binap), in the nanocages of C-FDU-12 was investigated by ³¹P-NMR characterization.

The liquid ³¹P-NMR spectrum of Ru-(*R*-Binap) and its solid-state magic-angle spinning ³¹P-NMR spectrum are shown in Fig. 4A. The isotropic chemical shifts at 56 ppm and -16.2 ppm could be identified by magic-angle spinning (Fig. 4Ab), which could be respectively assigned to the signals of the Ru-(*R*-Binap) and *R*-Binap ligand residues (excess *R*-Binap ligand was used for the synthesis of Ru-(*R*-Binap) according to a previous report³²). An asymmetric and broad peak was observed in the static ³¹P NMR spectrum of Ru-(*R*-Binap)@C-FDU-12 due to chemical-shift anisotropy of the ³¹P nucleus (Fig. 4Ba). Interestingly, the static ³¹P NMR spectrum of Ru-(*R*-Binap)@C-FDU-12 displays a sharp peak at 56 ppm in the presence of solvent (Fig. 4Bb), indicating that Ru-(*R*-Binap) could move in the nanocages of C-FDU-12. The

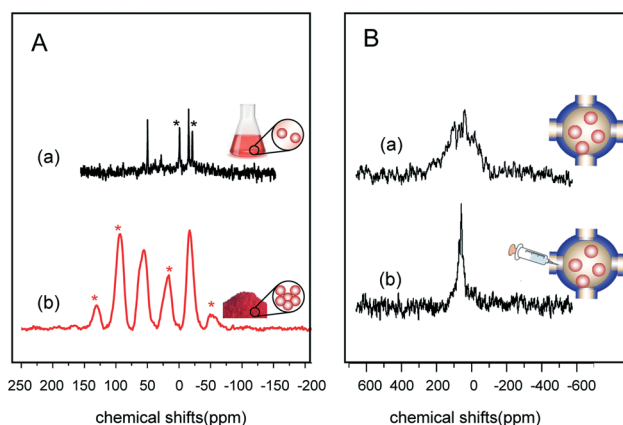


Fig. 4 (A) (a) Liquid ³¹P-NMR spectrum obtained under an inert atmosphere using degassed $CHCl_3$ as the solvent and (b) the solid-state magic-angle spinning (MAS) ³¹P-NMR spectrum of Ru-(*R*-Binap). (B) Static ³¹P-NMR spectra of Ru-(*R*-Binap)@C-FDU-12 (0.71 wt% Ru) (a) in the solid state and (b) in suspension with degassed $CHCl_3$ as the solvent.

static ³¹P-NMR spectra of Ru-(*R*-Binap)@C-FDU-12 in the presence of different amounts of solvent are summarized in Fig. 5. The peak firstly appears in the presence of 20 μ l of $CHCl_3$, corresponding to 40% of the cage volume filled with the solvent (based on the N_2 sorption results). As the amount of $CHCl_3$ increases, the peak at 56 ppm becomes sharper, and the intensity of the signal increases and reaches a maximum with a $CHCl_3$ amount of 50 μ l, corresponding to 100% of the cage volume filled with the solvent. It is worth mentioning that the peak at -16.2 ppm which belongs to *R*-Binap could hardly be observed in the ³¹P-NMR spectrum of Ru-(*R*-Binap)@C-FDU-12, indicating that the silylation with Ph_2Cl_2Si is very efficient and allows controllable modification of the pore entrance of C-FDU-12.

The NMR spectroscopic studies further confirm that Ru-(*R*-Binap) has been successfully encapsulated in the nanocage of C-FDU-12. Moreover, the confined Ru-(*R*-Binap) can move freely in the nanocages during a liquid phase catalytic process. Thus, Ru-(*R*-Binap)@C-FDU-12 is a solid catalyst as a whole, but has homogeneous properties on the nanoscale.

Asymmetric hydrogenation of β -keto esters

The catalytic performance of Ru-(*R*-Binap)@C-FDU-12 was investigated in the asymmetric hydrogenation of methyl acetoacetate. As shown in Table 2, no product was detected

Table 1 The textural parameters of C-FDU-12 and Ru-(*R*-Binap)@C-FDU-12 at different Ru content

Catalysts	Ru content/wt%	$S_{BET}/m^2 g^{-1}$	$V_p^a/cm^3 g^{-1}$	Cage size ^b /nm
Ru-(<i>R</i> -Binap)@C-FDU-12-0	0	381	0.49	9.1
Ru-(<i>R</i> -Binap)@C-FDU-12-0.12	0.12	26.4	0.048	8.0
Ru-(<i>R</i> -Binap)@C-FDU-12-0.28	0.28	17.9	0.034	8.0
Ru-(<i>R</i> -Binap)@C-FDU-12-0.37	0.37	18.1	0.038	8.0
Ru-(<i>R</i> -Binap)@C-FDU-12-0.5	0.5	8.2	0.017	8.0
Ru-(<i>R</i> -Binap)@C-FDU-12-0.71	0.71	6.6	0.016	8.0

^a Estimated from the amounts adsorbed at a relative pressure (P/P_0) of 0.99. ^b The pore size distribution calculated from the N_2 adsorption branch using the BJH method.

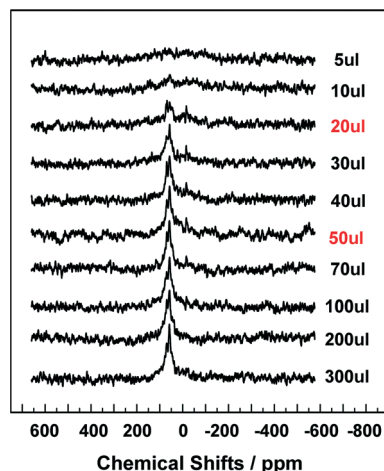


Fig. 5 ^{31}P -NMR spectra measured under static conditions of Ru-(*R*-Binap)@C-FDU-12 (0.71 wt% Ru) in the presence of different amounts of CHCl_3 .

with only C-FDU-12, showing that C-FDU-12 is not active for this reaction. Under the same reaction conditions, Ru-(*R*-Binap)@C-FDU-12-0.12 (0.12 wt% Ru) exhibits 99% yield with 96.5% ee, very close to those of its homogeneous counterpart. The high ee of Ru-(*R*-Binap)@C-FDU-12 suggests that the current encapsulation method does not cause damage to Ru-(*R*-Binap) during the silylation process. The TOF of Ru-(*R*-Binap) is still lower than that of the homogeneous Ru-(*R*-Binap). This is due to the mass diffusion limitation of the reactants and products through the nanocages. When the *S/C* increases to 2000, the yield and enantioselectivity of methyl-3-hydroxybutyrate do not significantly alter, while the TOF value becomes a little higher, as shown in entry 4. The influence of the catalyst loading amount on the catalytic performance of Ru-(*R*-Binap)@C-FDU-12 was also investigated (entries 3, 5–9). With the metal loading increasing from 0.12 wt% to 0.82 wt%, the molecular number of the metal complex in each cage increases from 7 to 45, and the TOF value of Ru-(*R*-Binap)@C-FDU-12 decreases from 299 h^{-1} to 82 h^{-1} , while the enantioselectivity nearly remains the same (Fig. 6).

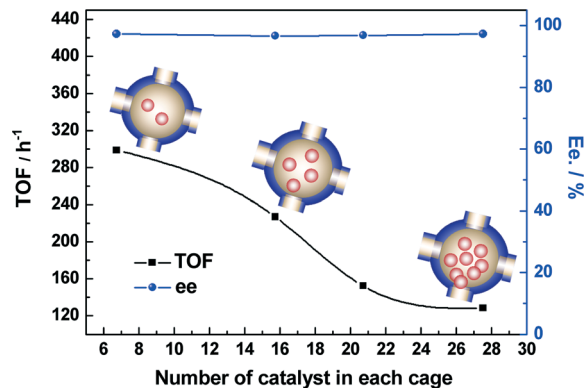


Fig. 6 TOF and ee values of MAA hydrogenation in the presence of Ru-(*R*-Binap)@C-FDU-12 with different numbers of Ru-(*R*-Binap) molecules in each nanocage.

As shown in Table 1, the BET surface area and pore volume of Ru-(*R*-Binap)@C-FDU-12 decrease as the Ru-(*R*-Binap) loading increases. Thus, the decreased activity is probably due to the crowded microenvironment in the nanocages caused by the high content of Ru-(*R*-Binap), which makes the diffusion of reactants and products difficult. The maintained enantioselectivity indicates that the properties of Ru-(*R*-Binap) remain unchanged regardless of the number of molecular catalyst encapsulated in the nanocages. Fig. 7 gives the kinetic plots of the asymmetric hydrogenation of methyl acetoacetate by Ru-(*R*-Binap)@C-FDU-12 with Ru content of 0.5 wt%. After the reaction was carried out for 3 h, the solid catalyst was filtered off, while the filtrate was stirred under the same conditions for another 21 h. However, the yield of the product remains almost the same as that measured at 3 h, confirming that the solid catalyst actually is responsible for the catalytic reaction.

Anyway, this encapsulation method enables the precise control of the loading amount of metal complexes in the nanocages to meet different needs. For some particular asymmetric catalytic system, the number of encapsulated metal complexes should be precisely adjusted to obtain high activity, e.g., one molecule per nanocage for the catalyst which may be

Table 2 Asymmetric hydrogenation of methyl acetoacetate (MAA) catalyzed by Ru-(*R*-Binap)@C-FDU-12 at different Ru loadings^a

Entry	Catalysts	Number of cat. per cage	<i>S/C</i>	TOF ^b / h^{-1}	Yield ^c /%	Ee ^c /%
1	C-FDU-12	—	—	—	0	—
2	Ru-(<i>R</i> -Binap)	—	1000	1101	99	97.1
3	Ru-(<i>R</i> -Binap)@C-FDU-12-0.12	7	1000	299	99	96.5
4	Ru-(<i>R</i> -Binap)@C-FDU-12-0.12	7	2000	382	97	93.0
5	Ru-(<i>R</i> -Binap)@C-FDU-12-0.28	16	1000	227	99	96.7
6	Ru-(<i>R</i> -Binap)@C-FDU-12-0.37	21	1000	152	99	96.9
7	Ru-(<i>R</i> -Binap)@C-FDU-12-0.5	28	1000	127	99	97.3
8	Ru-(<i>R</i> -Binap)@C-FDU-12-0.71	39	1000	100	99	96.7
9	Ru-(<i>R</i> -Binap)@C-FDU-12-0.82	45	1000	82	99	97

^a All of the reactions were carried out under a hydrogen pressure of 4 MPa in 1.0 mL methanol at 50 °C for 24 h. ^b TOFs were calculated at the initial 1 h. ^c Yield and ee values were determined by GC on a Supelco g-DEX 225 capillary column.

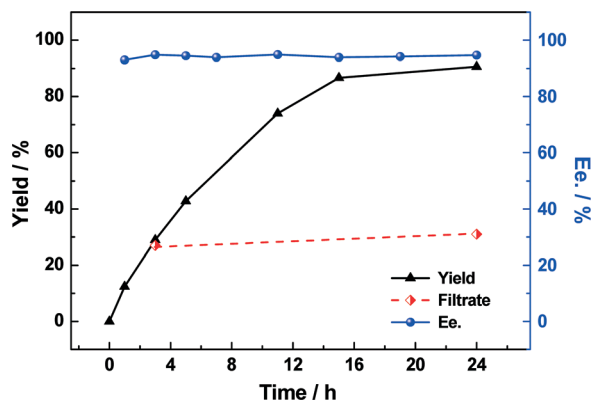


Fig. 7 Kinetic plots of the asymmetric hydrogenation of methyl acetoacetate by Ru-(*R*-Binap)@C-FDU-12 with Ru content of 0.5 wt%. The filtrate test was performed by removing the solid catalyst from the reaction system after 3 h.

deactivated by dimer formation (such as Ir-Binap), and two molecules or above for catalysts which show the cooperative activation effect (such as CoSalen).

The encapsulated catalyst was also used to catalyze the asymmetric hydrogenation of a wide range of β -keto esters for the production of different β -hydroxy esters, which are important intermediates in the fine chemical and pharmaceutical industries. As shown in Table 3, all of these substrates can be efficiently converted into the corresponding chiral alcohol by Ru-(*R*-Binap)@C-FDU-12 in high yield (91–99%) and high enantioselectivity (87–99% ee).

Ru-(*R*-Binap)@C-FDU-12 exhibits good catalytic stability and could be easily recycled by a simple filtration method. For the hydrogenation of methyl acetoacetate, the yield and enantioselectivity of the solid catalyst remain above 90% after four cycles (Fig. 8a). After the first cycle, 0.98 wt% Ru was found in the reaction filtrate by ICP analysis. After the second cycle, the amount of leaching species dropped down to 0.26 wt%, and a little amount of Ru species could be detected after the third cycle. The recycled solid catalyst could still maintain the

Table 3 Catalytic performance of Ru-(*R*-Binap)@C-FDU-12^a and homogeneous Ru-(*R*-Binap) for asymmetric hydrogenation of various β -keto esters^b

Entry	R	Yield ^c /%	Ee ^c /%
1	R ¹ = R ² = Me	99 (99)	97 (97.1)
2	R ¹ = Et, R ² = Me	99 (98.4)	98.8 (97.7)
3	R ¹ = <i>i</i> -Pr, R ² = Me	94.2 (97.8)	99 (99)
4	R ¹ = <i>t</i> -Bu, R ² = Me	99 (99)	99 (99)
5	R ¹ = -CH ₂ -Ph, R ² = Me	99 (99)	99 (99)
6	R ¹ = Me, R ² = Et	99 (99)	99 (99)
7	R ¹ = Me, R ² = <i>i</i> -Pr	91 (99)	87 (97)

^a Ru-(*R*-Binap)@C-FDU-12 with Ru content of 0.12 wt%. ^b All of the reactions were carried out under a hydrogen pressure of 4 MPa in 1.0 mL methanol at 50 °C with S:C = 1000:1. ^c The data in parentheses are for homogeneous Ru-(*R*-Binap).

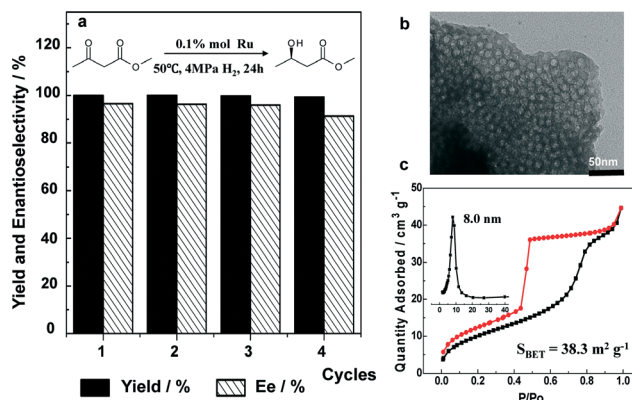


Fig. 8 (a) Recycling test of Ru-(*R*-Binap)@C-FDU-12 (0.12 wt% Ru) in the asymmetric hydrogenation of methyl acetoacetate, (b) the TEM image and (c) N₂ sorption isotherms of Ru-(*R*-Binap)@C-FDU-12 (0.12 wt% Ru) after cycling 4 times.

mesoporous structures of the fresh Ru-(*R*-Binap)@C-FDU-12 (Fig. 8b and c). The slight decrease in activity and enantioselectivity during the recycle process is considered to be partly caused by the air sensitivity of the catalytically active Ru-hydride species and partly due to the leaching of metal complexes.^{20,33}

Conclusions

In summary, we have developed an efficient method for the encapsulation of organic base sensitive metal complexes in the nanocages of mesoporous silica. With highly active chlorosilane, Ph₂Cl₂Si, as a silylating agent, the encapsulation could be performed at room temperature without any silylation catalysts. This method is proved to be available for the encapsulation of the Noyori catalyst Ru-(*R*-Binap) in the nanocages of C-FDU-12 without damaging Ru-(*R*-Binap). ³¹P-NMR results show that the encapsulated molecular catalyst could move freely in the nanocages during a liquid phase catalytic process. Thus, the intrinsic properties of Ru-(*R*-Binap) are preserved. Ru-(*R*-Binap)@C-FDU-12 exhibits excellent enantioselectivity which is comparable with that of its homogeneous counterpart for the asymmetric hydrogenation of β -keto esters and could be reused at least four times. We could expect that this encapsulation strategy would be generally applicable for the design of various high-efficient nanoreactors for the production of fine chemicals and pharmaceuticals.

Experimental section

Material information

Pluronic copolymer F127 (EO106PO70EO106) and [RuCl₂(benzene)]₂ were purchased from Sigma-Aldrich Company, USA. Dichlorodiphenylsilane (Ph₂Cl₂Si) was purchased from Beijing Coupling Technology Company Ltd, China. 2,2'-Bis(diphenylphosphino)-1,1'-binaphthyl ((*R*-Binap) was obtained from Shijiazhuang Shengjia Chemical Co, Ltd., China. Tetraethoxysilane (TEOS) was purchased from Shanghai Chemical Reagent Company of the Chinese Medicine Group. Methyl

acetoacetate and other β -keto esters were purchased from Alfa Aesar Company. All of the solvents were of analytical grade and deoxygenated by standard methods before use.

Preparation methods

The Ru-(*R*-Binap) complex was synthesized according to the literature method and was fully characterized by FT-IR (Fig. 2a), UV-vis (Fig. S3†), ^{31}P -NMR (Fig. 4), ^1H -NMR and ^{13}C -NMR spectroscopy (Fig. S1–S3†).³²

The mesoporous material FDU-12 was synthesized according to the literature method.³⁴ C-FDU-12 was obtained by carbonization of the as-made FDU-12 at 550 °C under a nitrogen atmosphere for 6 h.

The encapsulation was performed in a glove box. A typical process for the encapsulation of Ru-(*R*-Binap) in the nanocages of C-FDU-12 was as follows: C-FDU-12 (0.2 g) was evacuated at room temperature for 0.5 h. CH_2Cl_2 (0.5 mL) containing a given number of Ru-(*R*-Binap) was injected into the C-FDU-12 material under vacuum conditions with vigorous stirring. After evaporation of CH_2Cl_2 , 1 ml of dry hexane was injected into the resultant solid, followed by 0.5 ml of $\text{Ph}_2\text{Cl}_2\text{Si}$ (12 mmol g^{-1}). After reaction for 8 h under low pressure at room temperature, the resulting solid catalyst was isolated by filtration and thoroughly washed with CH_2Cl_2 . The Ru content of the encapsulated catalysts varied from 0.12 to 0.82 wt%. The number of Ru-(*R*-Binap) in each cage (n , Table 2) was calculated using the following equation:

$$n = \frac{N_{\text{Ru}(1\text{ g})} \times 6.02 \times 10^{23}}{\frac{V_{\text{mesopore}}}{\frac{4}{3}\pi\left(\frac{D}{2}\right)^3}}$$

$N_{\text{Ru}(1\text{ g})}$ is the mole of Ru-(*R*-Binap) per gram of the solid catalyst.

$V_{\text{mesop.}} = V_{\text{total}} - V_{\text{microp.}}$, where V_{total} means the total pore volume, $V_{\text{mesop.}}$ refers to the pore volume attributed by the mesopore and $V_{\text{microp.}}$ refers to the pore volume of the micropore.

D is the cage size of C-FDU-12.

Asymmetric hydrogenation of β -keto esters

A desired amount of the homogeneous or heterogeneous Ru-(*R*-Binap) catalyst (2 μmol) was added in an ampoule tube, followed by the addition of β -keto esters (2 mmol) and anhydrous methanol (1 mL). The ampoule tube was then transferred to a stainless steel autoclave and sealed. After purging with H_2 six times, the final H_2 pressure was adjusted to 4 MPa, and the reactor was heated to 323 K whilst vigorous stirring (700 rpm) for 24 h. After cooling down to room temperature, the H_2 pressure in the autoclave was released. The solid catalyst was separated by centrifugation and washed with 4 ml of MeOH. The filtrate was collected and analyzed by an Agilent 6890 GC equipped with a chiral Supelco γ -DEX 225 capillary column (30 m \times 0.25 mm \times 0.25 μm). The GC spectra of the

corresponding products hydrogenated by various β -keto esters were given in the ESI† (Fig. S4).

For recycling of the catalyst, the autoclave was opened in the glove box. After centrifugation under N_2 , the liquid was decanted, and the residual catalyst was washed thoroughly with CH_2Cl_2 , dried under vacuum and used directly for the next catalytic reaction.

Characterization

N_2 sorption isotherms were recorded on a Micromeritics ASAP2020 volumetric adsorption analyzer. Before the sorption measurements, the samples were degassed at 393 K for 6 h. X-Ray powder diffraction (XRD) patterns were recorded on a Rigaku RINT D/Max-2500 powder diffraction system using $\text{Cu K}\alpha$ radiation ($\lambda = 0.1541\text{ nm}$). Transmission electron microscopy (TEM) was performed using a FEI Tecnai G2 Spirit at an acceleration voltage of 120 kV. FT-IR spectra were collected using a Nicolet Nexus 470 IR spectrometer. All liquid and solid ^{31}P -NMR spectroscopy experiments were carried out at 9.4 T on a Varian Infinity Plus 400 spectrometer with a ^{31}P frequency of 161.83 MHz using a 5 mm Chemagnetic probe. One pulse sequence was used to collect ^{31}P liquid and solid NMR data, using a $\pi/2$ pulse width of 1.9 μs and a recycle delay of 10 s. The spinning rates in solid NMR experiments are 6 kHz and 7 kHz. The chemical shifts were referenced to $(\text{NH}_4)_2\text{HPO}_4$.

Ru-(*R*-Binap) (100 mg) in dried form was measured by MAS and static ^{31}P NMR spectroscopy. With the addition of different volumes of CHCl_3 (5 μL to 300 μL), the sample was kept for 30 min before it was subjected to detection by ^{31}P static NMR.

Acknowledgements

The authors would like to thank the Natural Science Foundation of China (21325313, 21232008 and 21273226) for financial support.

Notes and references

- Z. J. Jia, K. Jiang, Q. Q. Zhou, L. Dong and Y. C. Chen, *Chem. Commun.*, 2013, 49, 5892–5894.
- J. H. Wang, D. L. Liu, Y. G. Liu and W. B. Zhang, *Org. Biomol. Chem.*, 2013, 11, 3855–3861.
- A. E. Sheshenev, E. V. Boltukhina, A. J. P. White and K. K. Hii, *Angew. Chem., Int. Ed.*, 2013, 52, 6988–6991.
- S. K. Murphy and V. M. Dong, *J. Am. Chem. Soc.*, 2013, 135, 5553–5556.
- K. Li, N. F. Hu, R. S. Luo, W. C. Yuan and W. J. Tang, *J. Org. Chem.*, 2013, 78, 6350–6355.
- S. Xiang, Y. L. Zhang, Q. Xin and C. Li, *Chem. Commun.*, 2002, 2696–2697.
- P. Piaggio, P. McMorn, C. Langham, D. Bethell, P. C. Bulman, F. E. Hancock and G. J. Hutchings, *New J. Chem.*, 1998, 22, 1167–1169.
- N. Herron, *Inorg. Chem.*, 1986, 25, 4714–4717.

- 9 M. J. Sabater, A. Corma, A. Domenech, V. Fornes and H. Garcia, *Chem. Commun.*, 1997, 1285–1286.
- 10 A. Corma and H. Garcia, *Eur. J. Inorg. Chem.*, 2004, 1143–1164.
- 11 H. Q. Yang, L. Zhang, L. Zhong, Q. H. Yang and C. Li, *Angew. Chem., Int. Ed.*, 2007, **46**, 6861–6865.
- 12 H. Q. Yang, J. Li, J. Yang, Z. M. Liu, Q. H. Yang and C. Li, *Chem. Commun.*, 2007, 1086–1088.
- 13 B. Li, S. Y. Bai, X. F. Wang, M. M. Zhong, Q. H. Yang and C. Li, *Angew. Chem., Int. Ed.*, 2012, **51**, 11517–11521.
- 14 H. Q. Yang, L. Zhang, P. Wang, Q. H. Yang and C. Li, *Green Chem.*, 2009, **11**, 257–264.
- 15 B. Li, S. Y. Bai, P. Wang, H. Q. Yang, Q. H. Yang and C. Li, *Phys. Chem. Chem. Phys.*, 2011, **13**, 2504–2511.
- 16 S. Y. Bai, B. Li, J. Peng, X. M. Zhang, Q. H. Yang and C. Li, *Chem. Sci.*, 2012, **3**, 2864–2867.
- 17 S. Y. Bai, H. Q. Yang, P. Wang, J. S. Gao, B. Li, Q. H. Yang and C. Li, *Chem. Commun.*, 2010, **46**, 8145–8147.
- 18 X. Liu, S. Y. Bai, Y. Yang, B. Li, B. Xiao, C. Li and Q. H. Yang, *Chem. Commun.*, 2012, **48**, 3191–3193.
- 19 A. Miyashita, H. Takaya, K. Toriumi, T. Ito, T. Souchi and R. Noyori, *J. Am. Chem. Soc.*, 1980, **102**, 7932–7934.
- 20 A. G. Hu, H. L. Ngo and W. B. Lin, *J. Am. Chem. Soc.*, 2003, **125**, 11490–11491.
- 21 A. G. Hu, H. L. Ngo and W. B. Lin, *Angew. Chem., Int. Ed.*, 2003, **42**, 6000–6003.
- 22 A. G. Hu, S. Liu and W. B. Lin, *RSC Adv.*, 2012, **2**, 2576–2580.
- 23 A. G. Hu, G. T. Yee and W. B. Lin, *J. Am. Chem. Soc.*, 2005, **127**, 12486–12487.
- 24 P. Y. Wang, X. Liu, J. Yang, Y. Yang, L. Zhang, Q. H. Yang and C. Li, *J. Mater. Chem.*, 2009, **19**, 8009–8014.
- 25 A. B. Dongil, B. Bachiller-Baeza, A. Guerrero-Ruiz and I. Rodriguez-Ramos, *Catal. Commun.*, 2012, **26**, 149–154.
- 26 Q. Sun, X. J. Meng, X. Liu, X. M. Zhang, Y. Yang, Q. H. Yang and F. S. Xiao, *Chem. Commun.*, 2012, **48**, 10505–10507.
- 27 A. L. Monteiro, F. K. Zinn, R. F. deSouza and J. Dupont, *Tetrahedron: Asymmetry*, 1997, **8**, 177–179.
- 28 T. Floris, P. Kluson, L. Bartek and H. Pelantova, *Appl. Catal., A*, 2009, **366**, 160–165.
- 29 J. Theuerkauf, G. Francio and W. Leitner, *Adv. Synth. Catal.*, 2013, **355**, 209–219.
- 30 T. Deschner, Y. C. Liang and R. Anwender, *J. Phys. Chem. C*, 2010, **114**, 22603–22609.
- 31 J. Fan, C. Z. Yu, J. Lei, Q. Zhang, T. C. Li, B. Tu, W. Z. Zhou and D. Y. Zhao, *J. Am. Chem. Soc.*, 2005, **127**, 10794–10795.
- 32 M. Kitamura, T. Ohkuma and R. Noyori, *Org. Synth.*, 1998, **9**, 589.
- 33 A. R. McDonald, C. Muller, D. Vogt, G. P. M. van Klink and G. van Koten, *Green Chem.*, 2008, **10**, 424–432.
- 34 J. Fan, C. Z. Yu, F. Gao, J. Lei, B. Z. Tian, L. M. Wang, Q. Luo, B. Tu, W. Z. Zhou and D. Y. Zhao, *Angew. Chem., Int. Ed.*, 2003, **42**, 3146–3150.